Evidence for direct CFTR inhibition by CFTRinh-172 based on arginine 347 mutagenesis

Emanuela Caci, Antonella Caputo, Alexandre Hinzpeter, Nicole Arous, Pascale Fanen, Nitin D Sonawane, Alan S Verkman, Roberto Ravazzolo, Olga Zegarra-Moran, Luis Jv Galietta

Evidence for direct CFTR inhibition by $CFTR_{inh}$-172 based on arginine 347 mutagenesis

Emanuela Caci [*], Antonella Caputo [*], Alexandre Hinzpeter [†], Nicole Arous [†], Pascale Fanen [†], Nitin Sonawane [#], A.S. Verkman [#], Roberto Ravazzolo [*], Olga Zegarra-Moran [*], Luis J.V. Galietta [*¶]

* Laboratorio di Genetica Molecolare, Istituto Giannina Gaslini, L.go Gerolamo Gaslini 5, 16147 Genova, Italy

† INSERM, U841, IMRB, Dept. Génétique, and Université Paris 12, Faculté de Médecine, IFR10, Créteil, F-94000, France

Dept. of Medicine and Physiology, University of California, San Francisco, California

¶ Centro di Biotecnologie Avanzate, L.go Rosanna Benzi 10, 16132 Genova, Italy

Short title: Altered inhibition by $CFTR_{inh}$-172 in mutant CFTR

Corresponding author:
Luis J.V. Galietta
Laboratorio di Genetica Molecolare
Istituto Giannina Gaslini
16148 Genova, ITALY
Phone: (+39) 010-5636711; FAX: (+39) 010-3779797; E-mail: galietta@unige.it

SYNOPSIS

The cystic fibrosis transmembrane conductance regulator (CFTR) is an epithelial Cl^- channel inhibited with high affinity and selectivity by the thiazolidinone compound $CFTR_{inh}$-172. Here, we present evidence that $CFTR_{inh}$-172 acts directly on CFTR. We introduced mutations in amino acid residues of the sixth transmembrane helix of the CFTR protein, a domain that has an important role in the formation of the channel pore. Basic and hydrophilic amino acids at positions 334 – 352 were replaced with alanine and the sensitivity to $CFTR_{inh}$-172 was assessed using functional assays. We found that arginine to alanine change at position 347 reduced by 20 – 30 fold the inhibitory potency of $CFTR_{inh}$-172. Mutagenesis of arginine 347 to other amino acids also decreased inhibitory potency, with aspartate producing near total loss of $CFTR_{inh}$-172 activity. Our results provide evidence that $CFTR_{inh}$-172 interacts directly with CFTR, and that arginine 347 is important for the interaction.

Keywords: CFTR, cystic fibrosis, chloride channel, channel blocker, mutagenesis

Abbreviations: CFTR, cystic fibrosis transmembrane conductance regulator; NBD, nucleotide binding domain; TMD, transmembrane domain; YFP, yellow fluorescent protein

INTRODUCTION

The cystic fibrosis transmembrane conductance regulator (CFTR) protein is a Cl^- channel that has been studied extensively because of its involvement in the genetic disease cystic fibrosis and its pathogenic role in secretory diarrheas [1,2]. CFTR is composed of 12 transmembrane domains (TMDs), two nucleotide-binding domains (NBDs), and a cytosolic R region that contains multiple sites for cAMP-dependent phosphorylation [3,4]. Transport of anions through the transmembrane helices is controlled by the NBDs. It is believed that these structures interact with two molecules of ATP to form a dimer and that binding/hydrolysis of ATP molecules control CFTR channel opening [5].

In contrast to cation channels, which are characterized by a wide panel of specific and potent blockers, including natural toxins, anion channels are sensitive to a limited number of non-selective inhibitors that have relatively low potencies. Regarding CFTR, previously known inhibitors, including glibenclamide, niflumic acid, and diphenylamine-2-carboxylic acid, have low potency and poor selectivity [1,6]. High-throughput screening of large chemical libraries has allowed the discovery of more selective CFTR inhibitors [2]. So far, inhibitors with two chemical scaffolds have been identified: the thiazolidinone $CFTR_{inh}$-172 [7] and the glycine hydrazide GlyH-101 [8]. The former compound reduces CFTR activity at nanomolar concentrations in a voltage-independent manner by increasing the time spent in the closed state [9]. The latter is an open channel blocker, acting from the extracellular side to occlude the channel pore. Other recently discovered CFTR inhibitors include alpha-aminoazaheterocycle-methylglyoxal adducts [10] and a peptide toxin [11].

The mechanism and site of action of $CFTR_{inh}$-172 are unknown. Experiments indicating that $CFTR_{inh}$-172 is not effective on other ion channels and transporters suggested that it may be a direct inhibitor of the CFTR protein [7]. Based on its lack of voltage-dependence (despite its negative charge in solution) and the effect on CFTR kinetics (closed state stabilization), we postulated that $CFTR_{inh}$-172 is not an open channel blocker but an inhibitor of channel gating [9]. Since CFTR gating is controlled by NBDs, we hypothesized that $CFTR_{inh}$-172 binds to a site located within these protein domains. However, NBD mutants like G551D, G1349D, or P574H, do not show an altered sensitivity to $CFTR_{inh}$-172 [9,12]. In contrast, the potency of CFTR activators, whose effect involves direct interaction with the NBDs, is greatly altered by mutations like G551D which resides in NBD1 [13-15]. Therefore, we considered the possibility that $CFTR_{inh}$-172 binds to other regions of CFTR protein. In the present study, we have performed an alanine scanning of the sixth TMD, a CFTR structure that is important in the formation of CFTR pore and in anion transport [16-19]. We found that mutation of arginine 347 remarkably reduces CFTR sensitivity to $CFTR_{inh}$-172.

EXPERIMENTAL

Cell culture

Fisher rat thyroid (FRT) epithelial cells were cultured on plastic in Coon's modified F12 medium supplemented with 5% FCS, 2 mM L-glutamine, 100 U/ml penicillin and 100 µg/ml streptomycin. COS-7 cells were instead cultured in DMEM/F12 (1:1) medium with 10% FCS, 2 mM L-glutamine, 100 U/ml penicillin and 100 µg/ml streptomycin. HEK 293 cells were grown in Dulbecco's modified Eagle's medium (DMEM with Glutamax) containing 10% fetal calf serum, 100 U/ml penicillin and 100 µg/ml streptomycin.

CFTR mutagenesis

Mutations were introduced into a pcDNA3.1 plasmid carrying the wild type CFTR coding sequence using the QuickChange XL Site-Directed Mutagenesis Kit (Stratagene) following the manufacturer's instruction. The CFTR coding sequence was fully sequenced to confirm the mutagenesis reaction and to exclude the presence of undesired mutations.

CFTR microfluorimetric functional assay

CFTR functional assay was performed on transiently transfected COS-7 cells using the halide-sensitive yellow fluorescent protein YFP-H148Q/I152L [20]. Accordingly, COS-7 cells were seeded in 96-well microplates (25,000 cells/well) in 100 µl of antibiotic-free culture medium. After 6 hours, cells were co-transfected with pcDNA3.1 plasmids carrying the coding sequence for CFTR (wild type or mutant) and for the halide-sensitive YFP. The transfection reagent was Lipofectamine 2000 (Invitrogen). For each well, 0.2 µg of plasmid DNA and 0.5 µl of Lipofectamine 2000 were first pre-mixed in 50 µl of OPTI-MEM (Invitrogen) to generate transfection complexes, and then added to the cells. After 24 hours, the complexes were removed by replacement with fresh culture medium. The CFTR functional assay was performed after further 24 hours. For this purpose, the cells were washed two times with PBS and incubated for 20 – 30 minutes with 60 µl PBS containing forskolin (20 µM) with and without $CFTR_{inh}$-172 at various concentrations. After incubation, cells were transferred to an Olympus IX 50 fluorescence microscope equipped with a 20X objective, optical filters for detection of EYFP fluorescence (Chroma; excitation: HQ500/20X, 500 ± 10 nm; emission: HQ535/30M, 535 ± 15 nm; dichroic: 515 nm) and a photomultiplier tube (Hamamatsu). For each well, cell fluorescence was continuously measured before and after addition of 165 µl of a modified PBS containing 137 mM NaI instead of NaCl (final NaI concentration in the well: 100 mM). Where needed, the added solution contained $CFTR_{inh}$-172 at the same concentration present in the well. The output from the photomultiplier tube was digitized using a PowerLab 2/25 acquisition system (ADInstruments) and stored on a Macintosh computer. After background subtraction, cell fluorescence recordings were normalized for the initial average value measured before addition of I^-. The signal decay caused by YFP fluorescence quenching was fitted with a double exponential function to derive the maximal slope that corresponds to initial influx of I^- into the cells [15,21]. Maximal slopes were converted to rates of variation of intracellular I^- concentration (in mM/s) using the equation:

$$d[I^-]/dt = K_I[d(F/F_0)/dt]$$

where K_I is the affinity constant of YFP for I^- [20], and F/F_0 is the ratio of the cell fluorescence at a given time vs. initial fluorescence. Initial fluorescence values were similar among cells transfected with different CFTR constructs. This finding allowed us to conclude that differences in I^- influx were due to intrinsic differences in halide transport ability of CFTR mutants and not to changes in cell density or transfection efficiency.

Stable transfections

FRT cells expressing the yellow fluorescent protein YFP-H148Q/I152L were plated on 60 mm Petri dishes and transfected with the CFTR plasmids using Lipofectamine 2000. Cell clones co-expressing both CFTR and YFP proteins were generated by continuous selection with 0.5 mg/ml of Hygromycin B and 0.75 mg/ml of G418. Positive clones were identified by performing the CFTR functional assay in a microplate reader, as previously described [21].

CFTR protein analysis: transient transfection and immunoprecipitation/western blot

All cells were grown on 60 or 100 mm diameter dishes. Subconfluent cells (60%) were transfected by lipofection using LipofectAMINE® and Plus reagent (Invitrogen) according to the manufacturer's instructions. Confluent monolayers were harvested and used 24 hours post-transfection for immunoprecipitation.

Cells grown on 100 mm diameter dishes were harvested 24 h after transfection in PBS 1X, pelleted at 2,000 g at 4°C for 10 min, and then resuspended in 600 µl of cold of cold lysis buffer (20 mM Hepes pH 7, 150 mM NaCl, 1 mM EDTA and 1% Igepal, all from Sigma) supplemented with complete protease inhibitors (Roche Applied Sciences) for 30 min at 4°C. Cell lysates were

spun at 20,000 g for 15 min at 4 °C to pellet insoluble material. Supernatants were "pre-cleared" three times with Pansorbin cells (Calbiochem) and 150 µl of RIPA 5X (250 mM Tris-HCl pH 7.5, 750 mM NaCl, 5% Triton X-100, 5% Na-deoxycholate, 0.5% SDS) were added before addition of 0.8 µg of mAb 24-1 (R&D System) overnight at 4°C on a rotating wheel. A total of 25 µl of Pansorbin cells were added to the lysates and the incubation continued for one more hour at 4°C. They were spun at 12,000 g for 1 min at 4°C and the pellets were washed 3 additional times with RIPA 1X. Pellets were resuspended in ESB buffer (125 mM Tris-HCl pH6.8, 5% SDS, 25% sucrose and 5% 2-mercaptoethanol), heated at 37 °C for 15 min and spun at 12,000 g for 5 min at 4 °C. The totality of the immunoprecipitated material was separated on a 7.5% SDS-PAGE and electroblotted from the gels to polyvinylidene difluoride membrane (GE Healthcare). CFTR was immunodetected using monoclonal antibody MM13-4 (1/1,000) followed by horseradish peroxidase-conjugated anti-mouse (1/50,000), and visualized by chemiluminescence with West Dura kit (Pierce Chemical, IL) according to the manufacturer's instructions. Direct recording of the chemiluminescence was performed using the CCD camera of the GeneGnome analyzer and quantification was achieved using the GeneTools software (Syngene BioImaging Systems, Synoptics Ltd; sold by Ozyme, St. Quentin-en-Yvelines, France).

Immunoprecipitation/PKA assay

Transiently transfected HEK cells grown on 60 mm diameter dishes were harvested 24 h post-transfection in PBS 1X, pelleted at 2,000 g at 4°C for 10 min, and then resuspended in 200 µl of cold lysis buffer supplemented with complete protease inhibitors (Roche Applied Sciences) for 30 min at 4 °C. After a preclear with Pansorbin cells, 50 µl of RIPA 5X were added and the CFTR protein was immunoprecipitated as described above with 0.4 µg of 24-1 mAb. For PKA assay, the immunoprecipitating proteins were phosphorylated *in vitro* with 5 units of the catalytic subunit of PKA (Promega) and 10 µCi [γ-^{33}P] ATP (GE Healthcare), separated by 5% SDS-PAGE, dried and autoradiographed. Radioactivity was quantitated by radioanalytic scanning (Molecular Dynamics PhosphoImager).

Transepithelial Cl^- current measurements

FRT cells expressing wild type or mutant CFTR were seeded at high density on Snapwell permeable supports (Corning Costar; 500,000 cells/insert). The culture medium was replaced every 48 hours on both apical and basolateral sides. After 4-7 days from plating, the Snapwell supports carrying the FRT monolayers were mounted in a home-made Ussing chamber-like system. The apical chamber was filled with a low-Cl^- containing solution (in mM): 65 NaCl, 65 Na-gluconate, 2.7 KCl, 1.5 KH_2PO_4, 2 $CaCl_2$, 0.5 $MgCl_2$, 10 glucose, 10 Na-Hepes (pH 7.4). The basolateral chamber was instead filled with (in mM): 130 NaCl, 2.7 KCl, 1.5 KH_2PO_4, 1 $CaCl_2$, 0.5 $MgCl_2$, 10 glucose, 10 Na-Hepes (pH 7.4). The basolateral membrane was permeabilized with 250 µg/ml amphotericin B for 30 minutes before starting the recording. Experiments were done at 37°C with a continuous bubbling with air on both sides.

Hemichambers were connected to a DVC-1000 voltage clamp (World Precision Instruments Inc.) via Ag/AgCl electrodes and 1 M KCl agar bridges. The transepithelial electrical potential difference was clamped at zero to measure CFTR Cl^- currents across the apical membrane.

Synthesis of zwitterionic analogue of $CFTR_{inh}$-172: 5-(1-Oxido-4-pyridinyl)methylene)-2-thioxo-3-[3-(trifluoromethyl)phenyl]-4-thiazolidinone (thiazo N-O)

A mixture of 2-thioxo-3-(3-trifluoromethyl phenyl)-4-thiazolidinone (55 mg, 0.2 mmol; synthesized as described before [22]), 4-pyridinecarboxaldehyde-1-oxide (25 mg, 0.2 mmol), and sodium acetate (10 mg) in glacial acetic acid (0.5 ml) was refluxed for 8 h. The solvent was evaporated, and the residue was crystallized from ethanol and further purified by normal phase flash

chromatography to yield 22 mg of a yellow powder (yield 29 %); mp: 209-210 °C (decomp); MS (ES+) (*m/z*): $[M+H]^+$ calculated for $C_{16}H_9F_3N_2O_2S_2$, 382.39, found 383.01.

Patch-clamp recordings

The whole-cell configuration of the patch-clamp technique was used to measure the effect of the effect of $CFTR_{inh}$-172 on CFTR Cl^- currents. Experiments were carried out on FRT cells with stable expression of wild type or R347A CFTR. Borosilicate glass pipettes were pulled on a vertical two steps puller to a final resistance of 1 – 3 MΩ measured in the working solution. Currents were recorded with an EPC-7 patch-clamp amplifier (List Medical) using PULSE software (Heka) and sampled at 2 kHz with an Instrutech ITC-16 AD/DA interface. Data were filtered at 1 kHz and analysis was done with IgorPro (Wavemetrics). The bath solution contained (in mM): 150 NaCl, 1 $CaCl_2$, 1 $MgCl_2$, 10 glucose, 10 mannitol, 10 Na-Hepes (pH 7.4). The pipette (intracellular) solution contained (in mM): 120 CsCl, 10 TEA-Cl, 0.5 EGTA, 1 $MgCl_2$, 40 mannitol, 10 Cs-HEPES and 1 mM MgATP (pH 7.3). To build current-to-voltage relationships, pulses to membrane voltages from –100 to 100 mV were applied in 20 mV steps from a holding potential of 0 mV. $CFTR_{inh}$-172 was applied by extracellular perfusion. All experiments were done at room temperature (22 – 24 °C).

Data analysis and statistics

Dose-response relationships from each experiment were fitted with the Hill equation using the Igor software (WaveMetrics) to calculate K_i and Hill coefficient. We did not test $CFTR_{inh}$-172 at concentrations higher than 50 µM due to limited solubility of this compound at high micromolar concentrations.

Data are reported as representative traces and as mean ± sem. To determine the significance of differences between groups of data, we used analysis of variance (ANOVA) by means of Statview software. Differences were considered statistically significant when $P < 0.01$.

RESULTS

Anion transport and sensitivity to $CFTR_{inh}$-172 in a series of CFTR point mutants was measured with the functional assay based on the halide-sensitive YFP. COS-7 cells were transiently co-transfected with the plasmids coding for the fluorescent protein and the wild type or mutant CFTR. Anion transport was determined from the rate of fluorescence decrease upon extracellular addition of a modified PBS containing I^- instead of Cl^-. Cells expressing wild type CFTR and stimulated with the cAMP-elevating agent forskolin showed a fast fluorescence decrease, as expected, due to the large CFTR-mediated influx of I^- which replaces intracellular Cl^- (Figure 1A). The rate of I^- influx was 45-fold greater than that in mock transfected cells (Figure 1B). Mutants of the sixth transmembrane domain showed different rates of anion transport. T338A and R347A were similar to wild type CFTR. R334A and S341A showed reduced anion transport though significantly greater than cells transfected with the fluorescent protein alone (Figure 1B). More marked was the effect of R352A, which showed undetectable levels of CFTR activity. This finding may depend on the observed ability of mutations to arginine 352 to strongly decrease CFTR single channel conductance [23]. The absence of function did not allow us to measure the potency of $CFTR_{inh}$-172 for the R352A mutant.

Anion transport was measured in the presence of $CFTR_{inh}$-172. As shown by representative traces and dose-response relationships (Figure 1A, C, D), most of the CFTR mutants showed sensitivity to $CFTR_{inh}$-172 comparable to that of the wild type protein with K_i around 1 – 3 µM (Table 1). The exception was R347A. This mutant showed a dramatic shift in sensitivity with a K_i of 44.98 ± 4.71 µM (Figure 1A, D and Table 1). We also introduced a mutation at position 349

(alanine replaced by serine). This amino acid change made the sequence of the sixth transmembrane domain identical to that of murine CFTR. The A349S mutant had anion transport ability (Figure 1B) and sensitivity to $CFTR_{inh}$-172 (K_i = 1.23 ± 0.41 μM, Table 1) similar to those of the wild type channel. This result is consistent with the strong $CFTR_{inh}$-172 inhibition of mouse CFTR [24].

We tested the effect of replacement of arginine 347 with other amino acids. As found for R347A, also the mutants R347C and R347D showed a normal rate of anion transport but altered sensitivity to $CFTR_{inh}$-172 (Figure 2A, B). Remarkably, arginine to aspartate change produced near total loss of $CFTR_{inh}$-172 activity (Figure 2B).

Because arginine 347 is believed to be involved in the formation of a salt bridge with aspartic acid 924 [25], we also tested the CFTR mutants D924A and D924R. Unfortunately, these mutants showed no detectable CFTR activity (Figure 2A). To further investigate the importance of the salt bridge, we generated a double mutant, R347D/D924R, in which the positions of the charged amino acids are inverted. Interestingly, in contrast to D924R, the double mutant was able to transport anions but showed a low sensitivity to $CFTR_{inh}$-172, with an estimated K_i greater than 50 μM (Figure 2A, B), similar to that of the single R347D mutant.

We evaluated the maturation of the D924R mutant by immunoprecipitation followed by western blot or *in vitro* phosphorylation (Figure 2C). Wild type protein and the R347D mutant showed a normal pattern of electrophoretic mobility with a prevalent abundance of the band C which represents the fully glycosylated mature form of CFTR. As expected, the trafficking mutant F508del was associated with the presence of only band B, the core-glycosylated immature form of CFTR (not shown). In contrast to R347D, the D924R mutation produced a partial defect in maturation, with increased band B intensity compared to band C. Interestingly, this defect seemed to be corrected in the double mutant R347D/D924R (Figure 2C).

We next determined the sensitivity of the arginine 347 mutants to $CFTR_{inh}$-172 by direct measurement of electrogenic Cl^- transport (Figure 3A-E). FRT cells were stable transfected with wild type, R334A, R347A, and R347D CFTR, and transepithelial Cl^- currents were measured. The R347A and R347D mutants showed significantly reduced sensitivity to $CFTR_{inh}$-172 compared to the wild type CFTR, thus confirming the results obtained with the fluorescence assay (Figure 3A, B, D). The calculated K_i for wild type CFTR, R347A, and R347D was 0.85 ± 0.13 μM (n = 8), 17.35 ± 3.90 μM (n = 13), and 53.10 ± 4.74 μM (n = 6), respectively (Figure 3E). The values for the two mutants were significantly higher than that of wild type CFTR ($P < 0.01$). For comparison, the sensitivity of the R334A mutant was not significantly altered (K_i = 0.50 ± 0.18 μM, n = 6; Figure 3C, E), in agreement with fluorescence assay data. Interestingly, the R347D mutant, although insensitive to $CFTR_{inh}$-172, was fully inhibited by the open channel blocker GlyH-101 (Figure 3D). Dose-responses carried out on wild type CFTR and R347D cells showed identical sensitivity to GlyH-101 with K_i of 5.02 ± 0.90 μM (n = 6) and 4.99 ± 0.66 μM (n = 6), respectively (Figure 4A – C).

We also tested the sensitivity of wild type and R347D to a zwitterionic, net neutral analog of $CFTR_{inh}$-172 analog, thiazo N-O, in which the carboxyphenyl group is replaced by an oxido-4-pyridinyl group (Figure 5A). Although less potent than $CFTR_{inh}$-172, the thiazo N-O compound caused a dose-dependent decrease of wild type CFTR currents (K_i = 31.42 ± 7.30 μM, n = 4), but very weak inhibition of the R347D mutant (Figure 5B, C).

Whole-cell patch-clamp experiments were carried out to further investigate the mechanism of action of $CFTR_{inh}$-172. Experiments on cells expressing wild type CFTR (n =6) showed large cAMP-activated currents that were inhibited by more than 90% with $CFTR_{inh}$-172 (5 μM; Figure 6A, B). The dependence of CFTR currents versus the applied membrane potential was linear and the extent of inhibition by $CFTR_{inh}$-172 was not affected by membrane potential, as previously described. In cells expressing R347A-CFTR (n = 6), cAMP stimulation elicited currents with a

moderate outward rectification of the current-voltage relationship (Figure 6C, D). Despite the use of a $CFTR_{inh}$-172 concentration an order of magnitude higher than the half-effective concentration for wild type CFTR, the Cl^- currents of the R347A mutant were only partially inhibited (Figure 6C, D). The summary of data in Fig. 5E shows that $CFTR_{inh}$-172 at 10 µM produced a ~ 50 % reduction of R347A currents whereas the inhibition of wild type currents at 5 µM was nearly total. The graph also shows that $CFTR_{inh}$-172 inhibition was not affected by the applied membrane potential.

DISCUSSION

The thiazolidinone $CFTR_{inh}$-172 is now widely used as a high affinity and selective inhibitor of the CFTR Cl^- channel [26-32]. However, its mechanism of action is unknown. It has been uncertain whether $CFTR_{inh}$-172 is a direct inhibitor of the CFTR protein or a modulator of an interacting regulatory protein. In the present study, we have analyzed the effect on $CFTR_{inh}$-172 activity of mutations in the sixth TMD of the CFTR protein. We introduced mutations in residues arginine 334, threonine 338, and serine 341, which are believed to be located in the narrowest part of CFTR pore, thus determining channel conductance and ion selectivity. We also introduced mutations in arginine 347 and arginine 352, which are reported to influence CFTR channel properties but are located more distantly from the channel pore, probably in a cytosolic vestibule. We found, using three different techniques, that mutagenesis of arginine 347 strongly reduced $CFTR_{inh}$-172 potency. Although, the absolute values of $CFTR_{inh}$-172 K_i were dependent on the type of experiment (with fluorescence assays giving the highest values), there was a consistent 20 – 30 fold loss of potency in the arginine 347 mutants compared to the wild type protein. In contrast, mutagenesis of arginine 334, threonine 338, and serine 341 did not significantly alter $CFTR_{inh}$-172 affinity. This finding is consistent with previous patch-clamp data showing that $CFTR_{inh}$-172 inhibition does not interact with the inner CFTR pore since its effect is not affected by transmembrane voltage. Furthermore, $CFTR_{inh}$-172 does not change the mean open time of CFTR channel, a behavior that would be expected for a blocker interacting with the pore.

Arginine 347 lies on the cytosolic part of the sixth TMD although it is not clear whether it is exposed to the solvent [17]. Arginine 347 was initially considered as an amino acid residue directly involved in the interaction of CFTR with permeating anions [33.34]. Indeed, mutagenesis of this residue caused a change in the anomalous mole fraction behavior of CFTR, i.e. in the intrinsic properties of channel conductance and selectivity. Nevertheless, a subsequent study has instead pointed out that arginine 347, together with aspartate 924, forms a salt bridge which is important in the determination of the CFTR channel structure [25]. We have investigated the importance of the R347-D924 salt bridge in the inhibitory activity of $CFTR_{inh}$-172. We removed the negative charge at position 924 by replacing aspartate with alanine or arginine. Unfortunately, these mutations abolished anion transport thus impeding determination of $CFTR_{inh}$-172 activity. Determination of CFTR protein electrophoretic mobility revealed that mutagenesis of D924 causes a partial impairment in maturation. Indeed, D924R causes a reduced amount of fully glycosylated protein (band C) that may indicate that the mutant protein is less stable. This defect may be responsible for the absence of ion transport function, through a reduction of protein in the plasma membrane and/or defective gating and conductance. Interestingly, when we generated the double mutant R347D/D924R, in which the positions of positive and negative charges are inverted but the salt bridge is maintained [25], we found that anion transport and CFTR protein maturation were rescued compared to single D924 mutants. On the other hand, we found that the double mutant R347D/D924R did not behave as the wild type CFTR in terms of $CFTR_{inh}$-172 sensitivity but was more similar to single R347 mutants. Therefore, we conclude that it is not the presence of the salt bridge but rather that of arginine at position 347 as required for $CFTR_{inh}$-172 inhibition activity.

To further investigate the role of arginine 347 in the $CFTR_{inh}$-172 mechanism-of-action, we tested an analog, thiazo N-O, having the carboxyphenyl moiety replaced by a zwitterionic, neutral

moiety. We hypothesized that the negatively charged carboxyl in $CFTR_{inh}$-172 interacts with the positive charge of arginine 347, such that the effects of arginine 347 mutations could be explained by loss of electrostatic attraction (R347A), or generation of electrostatic repulsion (R347D). Accordingly, the activity of the neutral thiazo N-O compound had to be less affected by the R347D mutation. However, the potency of this compound on the R347D mutant was reduced, as found for $CFTR_{inh}$-172, providing evidence against direct electrostatic interaction between the $CFTR_{inh}$-172 carboxyl and arginine 347.

The finding that a single amino acid change in the CFTR protein sequence alters $CFTR_{inh}$-172 potency has two interesting implications. It represents the first indication that $CFTR_{inh}$-172 is a direct inhibitor of CFTR, thus supporting its value as a tool of research to inhibit CFTR function selectively. Second, it indicates that $CFTR_{inh}$-172 may be a useful probe to investigate the CFTR structure-function relationship. Our results may imply that arginine 347 is directly involved in binding to $CFTR_{inh}$-172. Alternatively, giving the reported importance of arginine 347 in CFTR channel structure, and our results with the thiazo N-O analog, it is possible that the binding site lies elsewhere in the CFTR sequence and that replacement of arginine 347 has an allosteric effect. For example, R347D mutation has been shown to alter ATPase activity in NBDs [35], a finding that points out to strong conformational coupling between TMDs and NBDs. However, it is important to point out that in our experiments the R347D mutant, although being poorly inhibited by $CFTR_{inh}$-172, showed an unaltered sensitivity to GlyH-101, an open channel blocker acting from the extracellular side [8]. This finding indicates that arginine 347 mutations do not cause a gross disruption of the CFTR pore structure.

In theory, a compound causing CFTR Cl^- current inhibition may act in two ways: by occluding the channel pore or by impairing the channel gating [1]. Occlusion of the pore, as is the case of GlyH-101 [8], is characterized by shortening of the mean open time and voltage dependence of the block (if the blocking molecule is electrically charged). $CFTR_{inh}$-172 acts instead in a voltage-independent manner and by increasing the mean closed time [9]. This behavior is different from that of classical open channel blocker and more suggestive of a mechanism of action involving gating inhibition, probably by stabilizing the closed state. CFTR gating is controlled by events occurring at the NBDs, i.e. cycles of ATP binding/hydrolysis that are coupled with NBD dimerization. Such processes induce in turn changes in conformation of TMDs leading to opening of CFTR pore. In theory, $CFTR_{inh}$-172 may act at one of the steps coupling NBDs to TMDs. Our results, by showing a change in potency caused by arginine 347 mutations, indicate that $CFTR_{inh}$-172 interacts directly with CFTR. Future studies are needed to assess if $CFTR_{inh}$-172 binds to TMDs or whether the role of arginine 347 is indirect, and involves a binding site located more distantly in the CFTR protein, possibly in the NBDs.

Acknowledgements. We thank the support of Telethon-Italy (GGP05103), CIPE-Regione Liguria (Biofarma 2), the NIH (P30 DK072517), and Cystic Fibrosis Foundation Therapeutics. This work was also supported by public grants from Institut National de la Santé et de la Recherche Médicale (INSERM) and Chancellerie des Universités de Paris, and the French Association "Vaincre la Mucoviscidose".

REFERENCES

1 Hwang, T.C. and Sheppard, D.N. (1999) Molecular pharmacology of the CFTR Cl^- channel. Trends Pharmacol. Sci. **20**, 448-453

2 Verkman, A.S., Lukacs, G.L. and Galietta, L.J.V. (2006) CFTR chloride channel drug discovery – inhibitors as antidiarrheals and activators for therapy of cystic fibrosis. Curr. Pharm. Des. **12**, 2235-2247

3 Sheppard, D.N. and Welsh, M.J. (1999) Structure and function of the CFTR chloride channel. Physiol. Rev. **79**, S23-S45

4 Akabas, M.H. (2000) Cystic fibrosis transmembrane conductance regulator. Structure and function of an epithelial chloride channel. J. Biol. Chem. **275**, 3729-3732

5 Vergani, P., Lockless, S.W., Nairn, A.C. and Gadsby, D.C. (2005) CFTR channel opening by ATP-driven tight dimerization of its nucleotide-binding domains. Nature **433**, 876-880

6 Schultz, B.D., Singh, A.K., Devor, D.C. and Bridges, R.J. (1999) Pharmacology of CFTR chloride channel activity. Physiol. Rev. **79**, S109-S144

7 Ma, T., Thiagarajah, J.R., Yang, H., Sonawane, N.D., Folli, C., Galietta, L.J.V. and Verkman, A.S. (2002) Thiazolidinone CFTR inhibitor identified by high-throughput screening blocks cholera toxin-induced intestinal fluid secretion. J. Clin. Invest. **110**, 1651-1658

8 Muanprasat, C., Sonawane, N.D., Salinas, D., Taddei, A., Galietta, L.J.V. and Verkman, A.S. (2004) Discovery of glycine hydrazide pore-occluding CFTR inhibitors: mechanism, structure-activity analysis, and in vivo efficacy. J. Gen. Physiol. **124**, 125-137

9 Taddei, A., Folli, C., Zegarra-Moran, O., Fanen, P., Verkman, A.S. and Galietta, L.J.V. (2004) Altered channel gating mechanism for CFTR inhibition by a high-affinity thiazolidinone blocker. FEBS Lett. **558**, 52-56

10 Routaboul, C., Norez, C., Melin, P., Molina, M.C., Boucherle, B., Bossard, F., Noel, S., Robert, R., Gauthier, C., Becq, F. and Decout, J.L. (2007) Discovery of alpha-aminoazaheterocycle-methylglyoxal adducts as a new class of high-affinity inhibitors of cystic fibrosis transmembrane conductance regulator chloride channels. J. Pharmacol. Exp. Ther. **322**, 1023-1035

11 Fuller, M.D., Thompson, C.H., Zhang, Z.R., Freeman, C.S., Schay, E., Szakacs, G., Bakos, E., Sarkadi, B., McMaster, D., French, R.J., Pohl, J., Kubanek, J. and McCarty, N.A. (2007) State-dependent inhibition of CFTR chloride channels by a novel peptide toxin. J. Biol. Chem. (in press)

12 Pedemonte, N., Lukacs, G.L., Du, K., Caci, E., Zegarra-Moran, O., Galietta, L.J.V. and Verkman, A.S. (2005) Small-molecule correctors of defective deltaF508-CFTR cellular processing identified by high-throughput screening. J. Clin. Invest. **115**, 2564-2571

13 Zegarra-Moran, O., Romio, L., Folli, C., Caci, E., Becq, F., Vierfond, J.M., Mettey, Y., Cabrini, G., Fanen, P. and Galietta, L.J.V. (2002) Correction of G551D-CFTR transport defect in epithelial monolayers by genistein but not by CPX or MPB-07. Br. J. Pharmacol. **137**, 504-512

14 Pedemonte, N., Sonawane, N.D., Taddei, A., Hu, J., Zegarra-Moran, O., Suen, Y.F., Robins, L.I., Dicus, C.W., Willenbring, D., Nantz, M.H., Kurth, M.J., Galietta, L.J.V. and Verkman, A.S. (2005) Phenylglycine and sulfonamide correctors of defective delta F508 and G551D cystic fibrosis transmembrane conductance regulator chloride-channel gating. Mol. Pharmacol. **67**, 1797-1807

15 Pedemonte, N., Boido, D., Moran, O., Giampieri, M., Mazzei, M., Ravazzolo, R. and Galietta, L.J.V. (2007) Structure-activity relationship of 1,4-dihydropyridines as potentiators of the cystic fibrosis transmembrane conductance regulator chloride channel. Mol. Pharmacol. **72**, 197-207

16 Cheung, M. and Akabas, M.H. (1997) Locating the anion-selectivity filter of the cystic fibrosis transmembrane conductance regulator (CFTR) chloride channel. J. Gen. Physiol. **109**, 289-299
17 Dawson, D.C., Smith, S.S. and Mansoura, M.K. (1999) CFTR: mechanism of anion conduction. Physiol. Rev. **79**, S47-S75
18 McCarty, N.A. and Zhang, Z.R. (2001) Identification of a region of strong discrimination in the pore of CFTR. Am. J. Physiol. **281**, L852-L867
19 Ge, N., Muise, C.N., Gong, X. and Linsdell, P. (2004) Direct comparison of the functional roles played by different transmembrane regions in the cystic fibrosis transmembrane conductance regulator chloride channel pore. J. Biol. Chem. **279**, 55283-55289
20 Galietta, L.J.V., Haggie, P.M. and Verkman, A.S. (2001) Green fluorescent protein-based halide indicators with improved chloride and iodide affinities. FEBS Lett. **499**, 220-224
21 Galietta, L.J.V., Springsteel, M.F., Eda, M., Niedzinski, E.J., By, K., Haddadin, M.J., Kurth, M.J., Nantz, M.H. and Verkman, A.S. (2001) Novel CFTR chloride channel activators identified by screening of combinatorial libraries based on flavone and benzoquinolizinium lead compounds. J. Biol. Chem. **276**, 19723-19728
22 Sonawane, N.D., Muanprasat, C., Nagatani, R. Jr., Song, Y. and Verkman, A.S. (2005) In vivo pharmacology and antidiarrheal efficacy of a thiazolidinone CFTR inhibitor in rodents. J. Pharm. Sci. **94**, 134-143
23 Aubin, C.N. and Linsdell, P. (2006) Positive charges at the intracellular mouth of the pore regulate anion conduction in the CFTR chloride channel. J. Gen. Physiol. **128**, 535-545
24 Salinas, D.B., Pedemonte, N., Muanprasat, C., Finkbeiner, W.F., Nielson, D.W. and Verkman, A.S. (2004) CFTR involvement in nasal potential differences in mice and pigs studied using a thiazolidinone CFTR inhibitor. Am. J. Physiol. **287**, L936-L943
25 Cotton, J.F. and Welsh, M.J. (1999) Cystic fibrosis-associated mutations at arginine 347 alter the pore architecture of CFTR. Evidence for disruption of a salt bridge. J. Biol. Chem. **274**, 5429-5435
26 Li, H., Findlay, I.A. and Sheppard, D.N. (2004) The relationship between cell proliferation, Cl^- secretion, and renal cyst growth: a study using CFTR inhibitors. Kidney Int. **66**, 1926-1938
27 Bruscia, E.M., Price, J.E., Cheng, E.C., Weiner, S., Caputo, C., Ferreira, E.C., Egan, M.E. and Krause, D.S. (2006) Assessment of cystic fibrosis transmembrane conductance regulator (CFTR) activity in CFTR-null mice after bone marrow transplantation. Proc. Natl. Acad. Sci. USA **103**, 2965-2970
28 Fang, X., Song, Y., Hirsch, J., Galietta, L.J.V., Pedemonte, N., Zemans, R.L., Dolganov, G., Verkman, A.S. and Matthay, M.A. (2006) Contribution of CFTR to apical-basolateral fluid transport in cultured human alveolar epithelial type II cells. Am. J. Physiol. **290**, L242-L249
29 Wang, Y., Soyombo, A.A., Shcheynikov, N., Zeng, W., Dorwart, M., Marino, C.R., Thomas, P.J. and Muallem, S. (2006) Slc26a6 regulates CFTR activity in vivo to determine pancreatic duct HCO_3^- secretion: relevance to cystic fibrosis. EMBO J. **25**, 5049-5057
30 Liu, X., Luo, M., Zhang, L., Ding, W., Yan, Z. and Engelhardt, J.F. (2007) Bioelectric properties of chloride channels in human, pig, ferret, and mouse airway epithelia. Am. J. Respir. Cell. Mol. Biol. **36**, 313-323
31 Perez, A., Issler, A.C., Cotton, C.U., Kelley, T.J., Verkman, A.S. and Davis, P.B. (2007) CFTR inhibition mimics the cystic fibrosis inflammatory profile. Am. J. Physiol. **292**, L383-L395
32 Wolde, M., Fellows, A., Cheng, J., Kivenson, A., Coutermarsh, B., Talebian, L., Karlson, K., Piserchio, A., Mierke, D.F., Stanton, B.A., Guggino, W.B. and Madden, D.R. (2007) Targeting CAL as a negative regulator of deltaF508-CFTR cell-surface expression: an RNA interference and structure-based mutagenetic approach. J. Biol. Chem. **282**, 8099-8109

33 Tabcharani, J.A., Rommens, J.M., Hou, Y.X., Chang, X.B., Tsui, L.C., Riordan, J.R. and Hanrahan, J.W. (1993) Multi-ion pore behaviour in the CFTR chloride channel. Nature **366**, 79-82

34 Tabcharani, J.A., Linsdell, P. and Hanrahan, J.W. (1997) Halide permeation in wild-type and mutant cystic fibrosis transmembrane conductance regulator chloride channels. J. Gen. Physiol. **110**, 341-354

35 Kogan, I., Ramjeesingh, M., Huan, L.J., Wang, Y. and Bear, C.E. (2001) Perturbation of the pore of the cystic fibrosis transmembrane conductance regulator (CFTR) inhibits its ATPase activity. J. Biol. Chem. **276**, 11575-11581

FIGURE LEGENDS

Figure 1 Mutants of the sixth transmembrane domain
(**A**) Representative traces showing normalized cell fluorescence recordings and quenching upon I^- addition in COS-7 cells transfected with wild type (top) or R347A (bottom) CFTR. Experiments were performed after stimulation of CFTR with forskolin (20 μM) in the presence or absence of $CFTR_{inh}$-172 (10 μM). (**B**) Rate of I^- transport measured from experiments as in A in COS-7 cells transfected with the wild type or mutant CFTR. Cells were stimulated with forskolin in the absence of $CFTR_{inh}$-172. Wild type CFTR and all mutants except R352A showed an I^- influx significantly higher ($P < 0.01$) than mock-transfected cells. (**C – D**) Dose-response relationships determined for $CFTR_{inh}$-172 on wild type and mutant CFTR. Each point is the mean ± sem of 4 – 10 experiments.

Figure 2 Mutagenesis of R347 and D924 residues
(**A**) Rate of I^- transport measured in COS-7 cells transfected with the indicated constructs. In contrast to all other constructs, D924A and D924R did not show a significant I^- transport compared to mock-transfected cells. (**B**) $CFTR_{inh}$-172 dose-response relationships for wild type, R347D, and R347D/D924R CFTR. Each point is the mean ± sem of 4 – 10 experiments. (**C**) Analysis of CFTR protein maturation by immunoprecipitation/radioactive labeling (top panel) or by immunoprecipitation/western blot (middle panel). The position of mature fully glycosylated (band C) and immature core glycosylated (band B) CFTR is indicated. The bottom panel reports ratios of band C/(band C+ band B) intensities (mean ± sem) measured for the two types of experiments. Empty bars: immunoprecipitation/radioactive labeling; filled bars: immunoprecipitation/western blot (n = 3 for both conditions). The asterisks indicate a significant difference relative to wild type CFTR ($P < 0.01$).

Figure 3 CFTR Cl^- current inhibition by $CFTR_{inh}$-172
(**A – D**) Representative traces showing recordings of transepithelial Cl^- currents measured in FRT cells with stable expression of wild type, R347A, R334A, and R347D-CFTR. Cells were first stimulated with forskolin (20 μM) to activate CFTR and then tested with increasing concentrations of $CFTR_{inh}$-172. In **D**, GlyH-101 (25 μM) was added at the end of experiment to block remaining CFTR activity. (**E**) $CFTR_{inh}$-172 dose-response relationships obtained from experiments as in **A – D**. Each point is the mean ± sem of 6 – 13 experiments.

Figure 4 CFTR Cl^- current inhibition by GlyH-101
(**A**, **B**) Representative traces showing transepithelial Cl^- currents measured in FRT cells with stable expression of wild type, and R347D-CFTR. Cells were first stimulated with forskolin (20 μM) to activate CFTR and then tested with increasing concentrations of GlyH-101. (**C**) GlyH-101 dose-responses. Each point is the mean ± sem of 6 experiments.

Figure 5 CFTR Cl^- current inhibition by thiazo N-O
(**A**) Chemical structures of thiazo N-O and $CFTR_{inh}$-172. (**B**) Representative recordings showing effect of increasing concentrations of thiazo N-O on wild type and R347D activity. (**C**) Thiazo N-O dose-response. Each point is the mean ± sem of 4 experiments.

Figure 6 Patch-clamp analysis of CFTR inhibition by $CFTR_{inh}$-172

(**A**, **C**) Superimposed membrane currents recorded from cells expressing wild type and R347A CFTR at membrane potentials between –100 and +100 mV. Currents were recorded in the absence and in the presence of $CFTR_{inh}$-172 (5 μM for wild type, 10 μM for R347A). (**B**, **D**) Plots of current to voltage relationships for the experiments shown in A and C, respectively. (**E**) Summary of block caused by $CFTR_{inh}$-172 at all membrane potentials on wild type (at 5 μM) and R347A (at 10 μM). Data are mean ± sem (n = 6 for both wild type and R347A).

Table 1

Properties of wild type and mutant CFTR

	inh-172 K_i (μM)	*Hill coefficient*	*I^- influx (mM/s)*	*n*
Wild type	1.32 ± 0.25	1.03 ± 0.07	0.1336 ± 0.0107	10
S341A	0.57 ± 0.17	1.21 ± 0.37	0.0297 ± 0.0064	4
T338A	3.20 ± 0.86	1.13 ± 0.20	0.1260 ± 0.0225	4
R347A	44.98 ± 4.71 (**)	0.91 ± 0.04	0.1288 ± 0.0154	7
R334A	2.39 ± 0.74	0.93 ± 017	0.0313 ± 0.062	4
A349S	1.23 ± 0.41	1.11 ± 0.25	0.1500 ± 0.011	4
R347D	> 50		0.1160 ± 0.0136	7
R347D/D924R	> 50		0.1008 ± 0.0504	4
R347C	> 50		0.1437 ± 0.0123	4
mock			0.003 ± 0.001	10

Sensitivity to $CFTR_{inh}$-172 and I^- transport ability for wild type and mutant CFTR. Data obtained with the halide-sensitive YFP assay on transfected COS-7 cells. The table reports K_i and Hill coefficient (calculated by fitting $CFTR_{inh}$-172 dose-response relationships), maximal I^- influx values in the absence of inhibitor, and number of experiments. For all fits the correlation coefficient R^2 was higher or equal to 0.97. Asterisks (**) indicate that the R347A K_i was significantly higher ($P < 0.01$) compared to wild type CFTR. For R347 mutants other than R347A, sensitivity to $CFTR_{inh}$-172 was so low that K_i could not determined precisely (see Methods). I^- influx values for all CFTR constructs were significantly higher than mock-transfected cells ($P < 0.01$).

Biochemical Journal Immediate Publication. Published on 26 Mar 2008 as manuscript BJ20080029

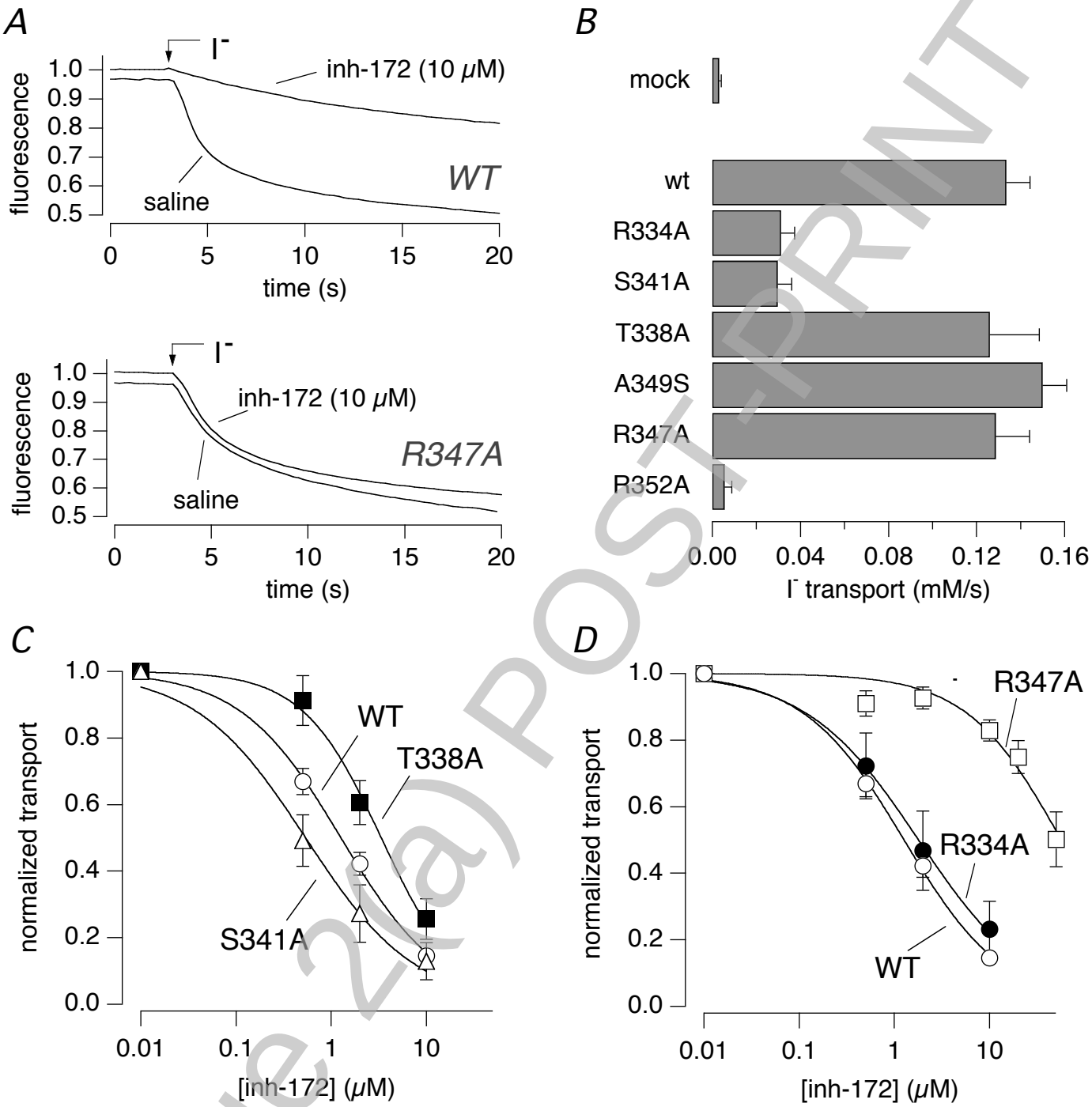

Figure 1

Biochemical Journal Immediate Publication. Published on 26 Mar 2008 as manuscript BJ20080029

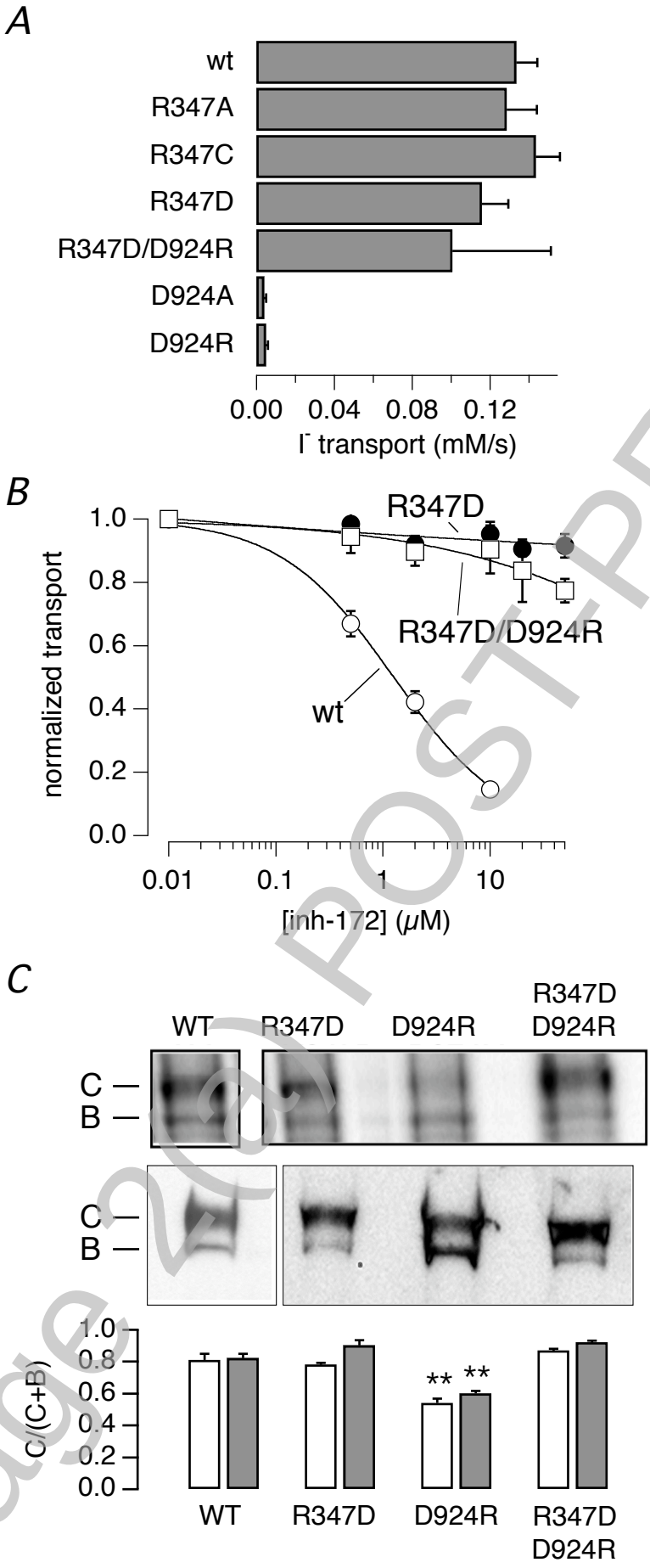

Figure 2

Biochemical Journal Immediate Publication. Published on 26 Mar 2008 as manuscript BJ20080029

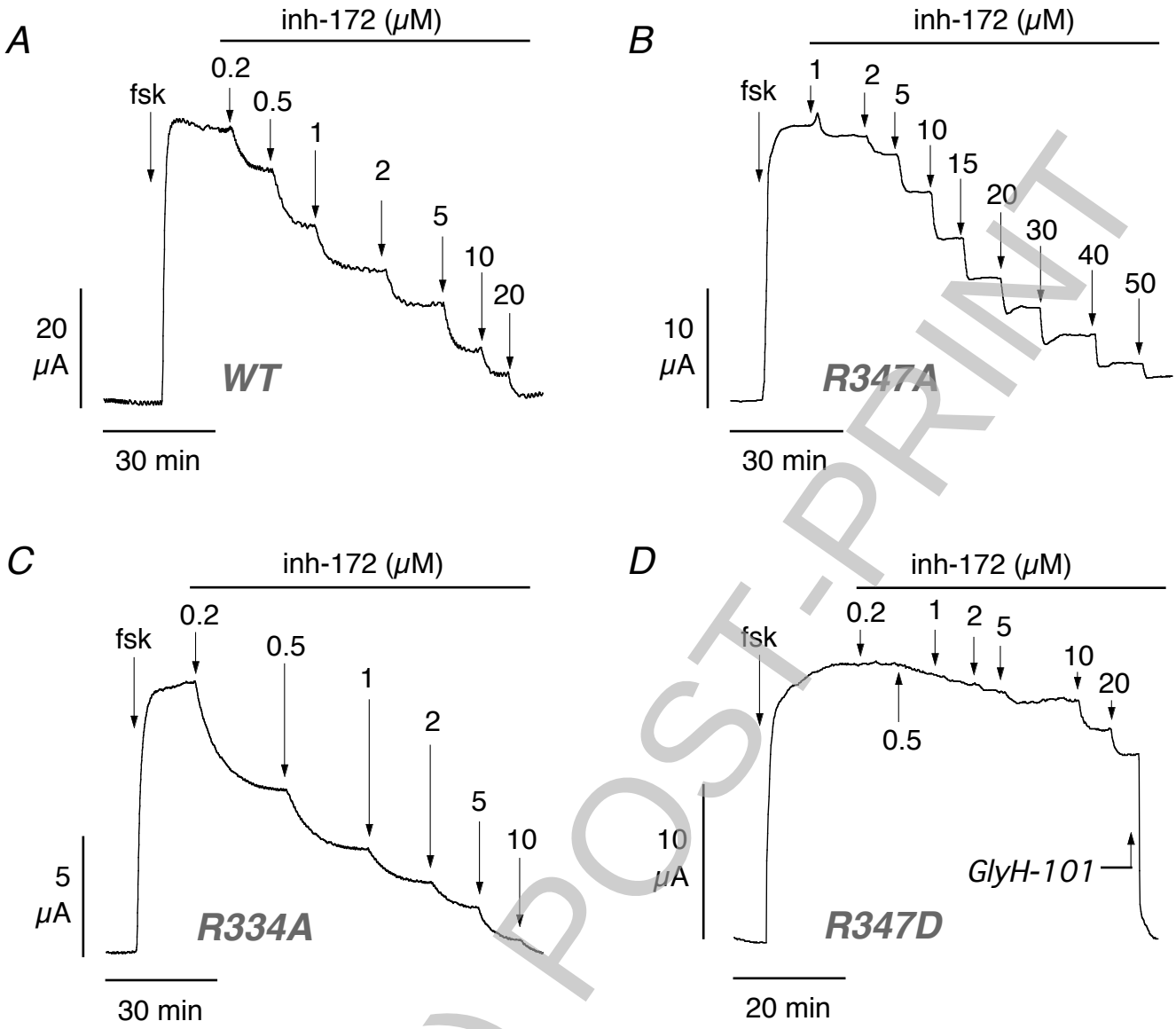

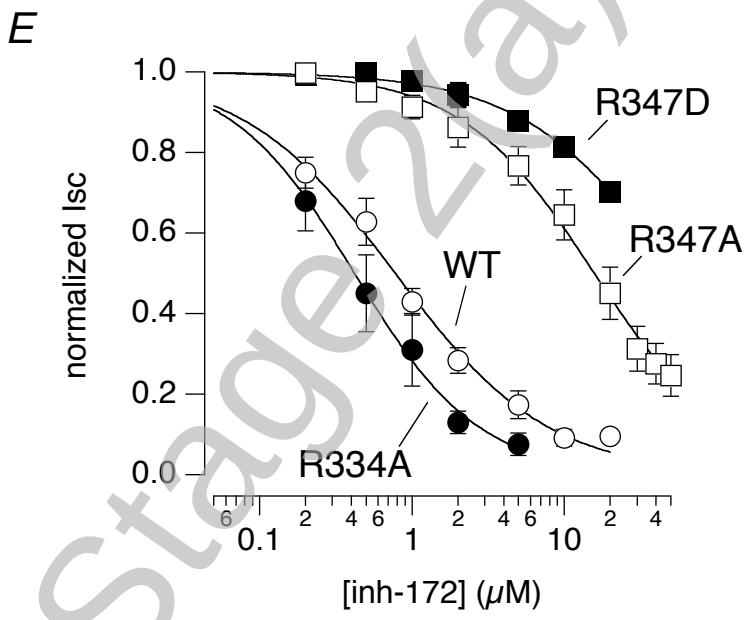

Figure 3

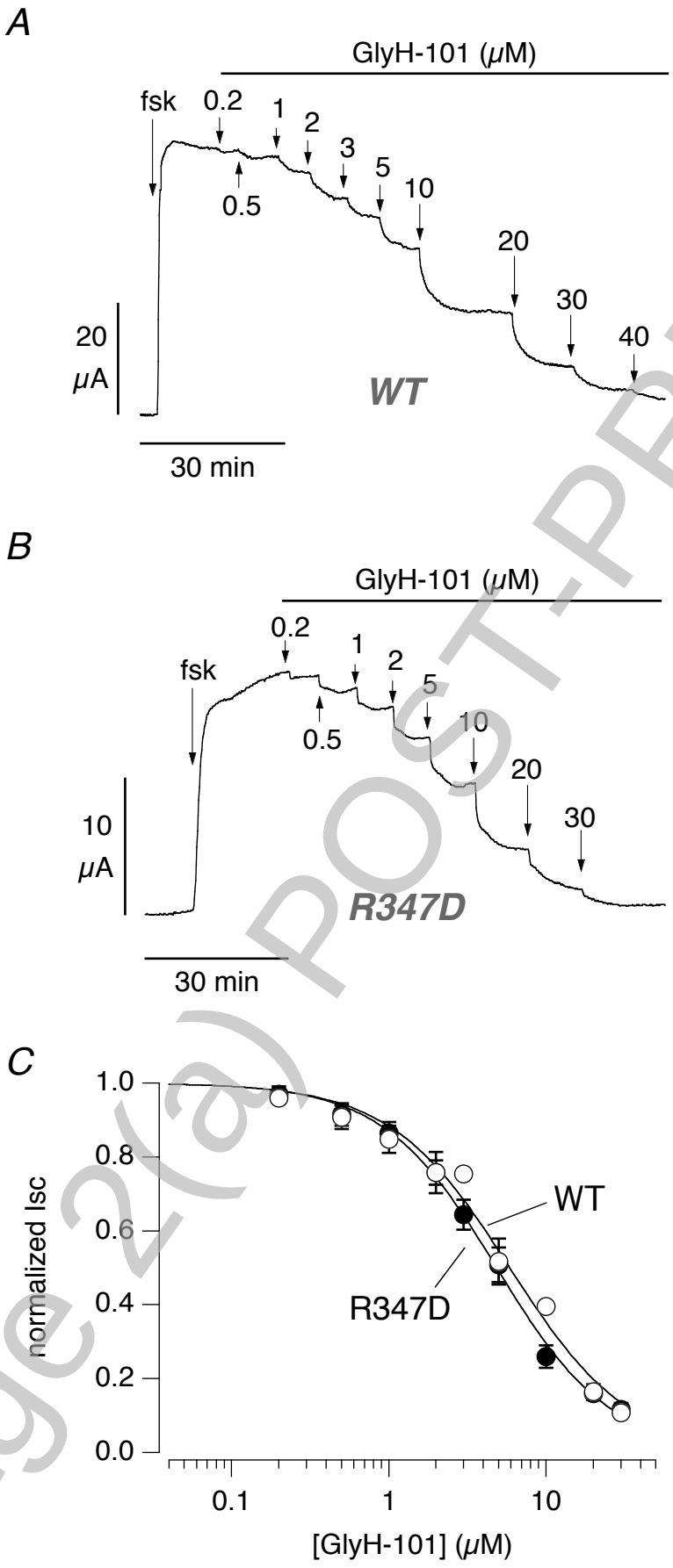

Figure 4

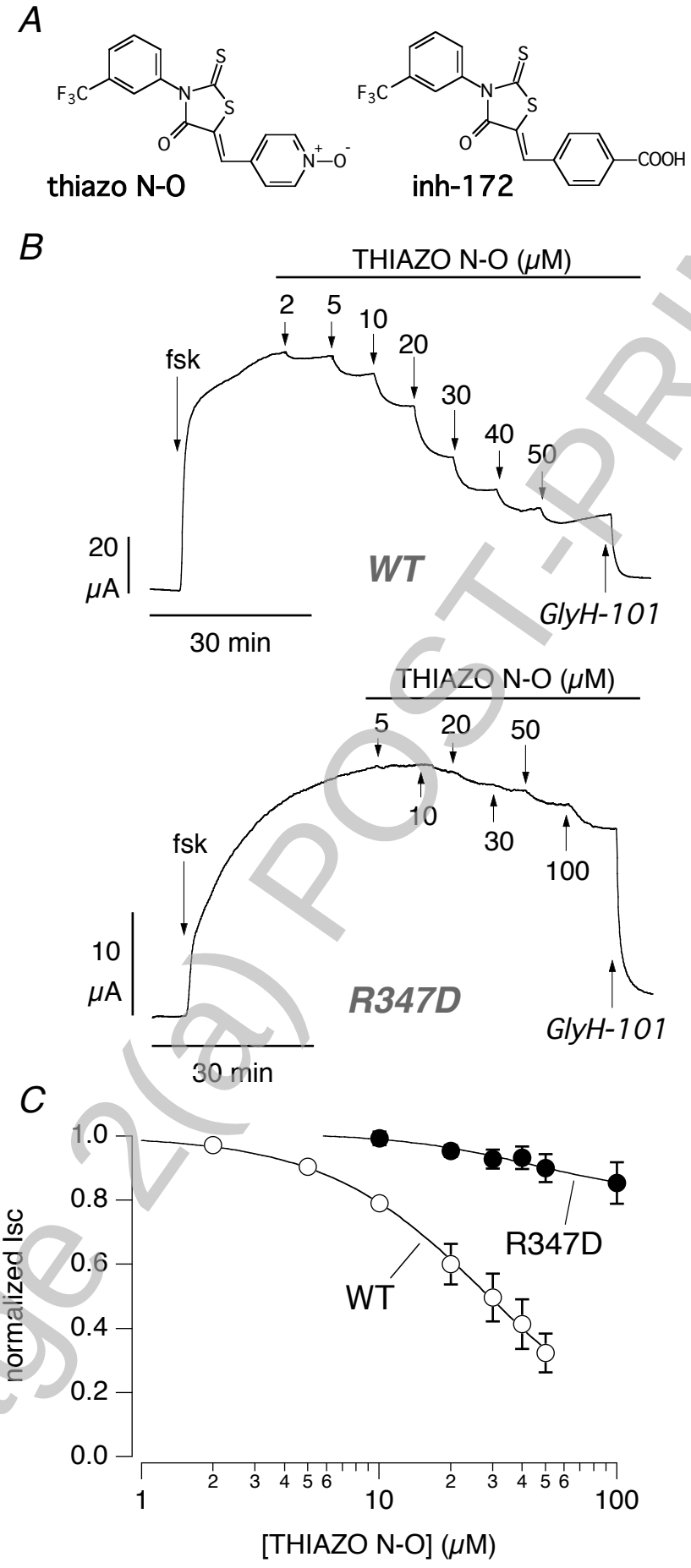

Figure 5

Biochemical Journal Immediate Publication. Published on 26 Mar 2008 as manuscript BJ20080029

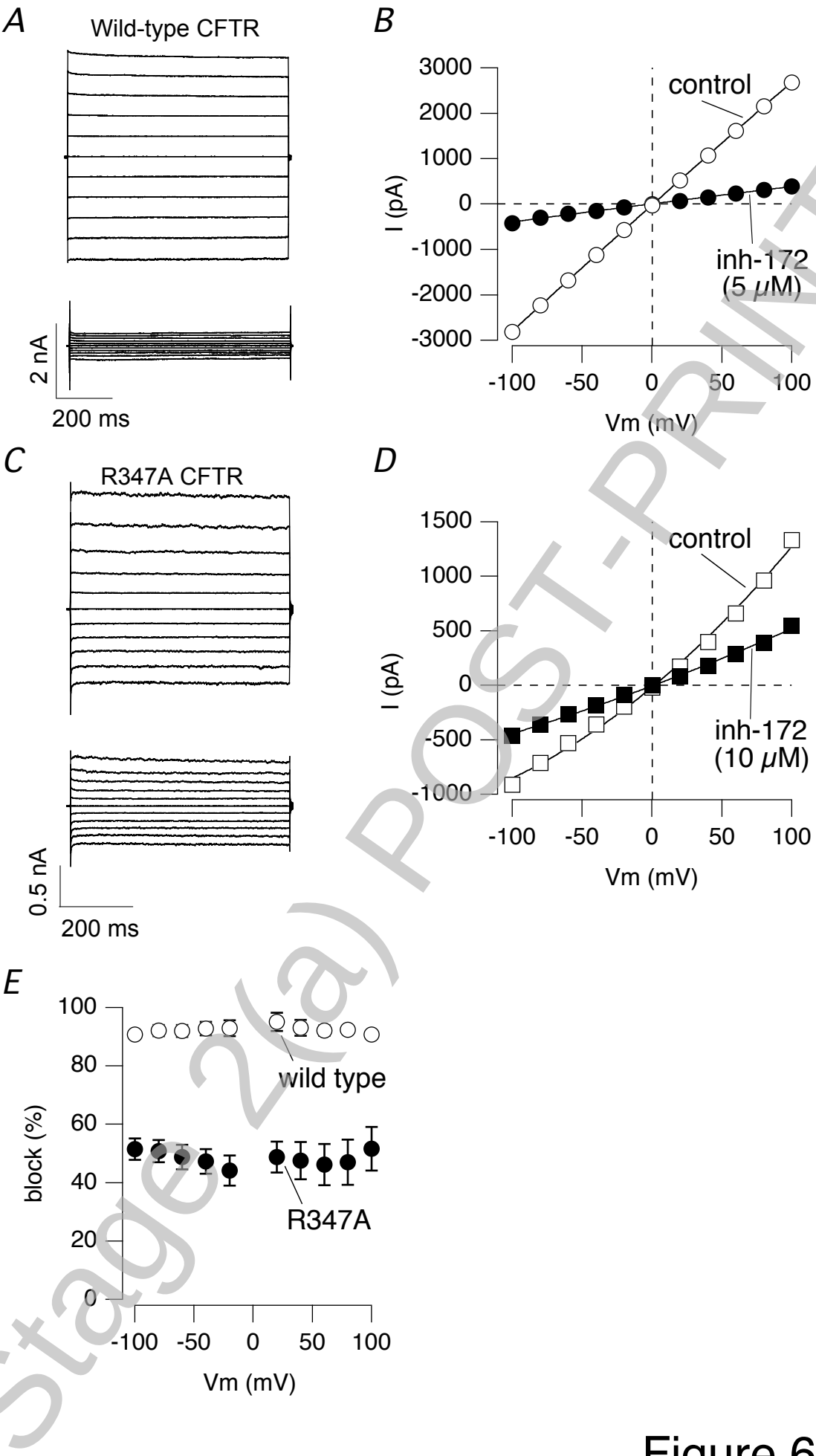

Figure 6